

Realtime Internal-Impedance Measurement of Lithium-ion Battery Using Discrete-Interval-Binary-Sequence Injection

Minh Tran

*Department of Electrical Engineering
Tampere University
Tampere, Finland
minh.tran@tuni.fi*

Tomi Roinila

*Department of Electrical Engineering
Tampere University
Tampere, Finland
tomi.roinila@tuni.fi*

Joni Markkula

*Department of Electrical Engineering
Tampere University
Tampere, Finland
joni.markkula@tuni.fi*

Abstract—Internal impedance of a Lithium-ion (Li-ion) battery is an important parameter in evaluating the battery characteristics such as the state-of-charge (SOC) and state-of-health (SOH). Recent studies have shown broadband methods based on pseudo-random binary sequence (PRBS) and Fourier techniques with which the battery impedance can be accurately and rapidly measured in real time. Applying the conventional PRBS requires, however, a relatively high injection amplitude that may easily interfere with the normal battery operation and produce nonlinear distortions. This paper proposes the use of a discrete-interval-binary sequence (DIBS) for a battery impedance measurement. The DIBS is a computer-optimized binary sequence in which the energy is maximized at specified harmonic frequencies to minimize the required level of signal injection. Otherwise the DIBS has the same attractive characteristics as the conventional PRBS. Experimental results based on a commercial Li-ion battery are presented to demonstrate the effectiveness of the proposed method.

Index Terms—batteries, energy storage, impedance measurement, realtime monitoring

I. INTRODUCTION

Lithium-ion (Li-ion) batteries have become widely used in many electronic and electric vehicle applications in recent years. This is due to their high energy and power density and continuously reducing prices [1]. However, constant monitoring of the battery state is required for guaranteeing a safe operation [2]. The battery state is often characterized by state parameters such as the state-of-charge (SOC) and state-of-health (SOH) which are typically indirectly estimated using the battery voltage, current and temperature.

Studies have shown that the Li-ion battery internal impedance provides direct information about the battery SOC and SOH [3], [4]. The impedance can be accurately and reliably obtained by electrochemical impedance spectroscopy (EIS) but the method is not well suited in practical applications due to difficult hardware implementation and long measurement time. Recent studies have applied broadband methods such as the pseudo-random binary sequence (PRBS) to measure the battery impedance [5]. In the method, the PRBS is placed on top of the battery nominal output current so that the battery is charged and recharged according to

the applied perturbation. The resulting terminal output current and output voltage are measured, and Fourier techniques are applied to extract the impedance information. As the PRBS is a broadband sequence, that is, the signal has energy at several frequencies, the impedance can be measured in a fraction of time compared to the EIS which is based on single sinusoidal injection. In addition, as the PRBS has a binary form, the sequence is very easy to implement in practice.

The drawback in using the PRBS in battery-impedance measurement is that the sequence energy is distributed over many harmonic frequencies. For an impedance measurement that requires a high signal-to-noise ratio (SNR), for example, due to strong external noise, either the injection amplitude has to be increased, or more periods of injection and averaging have to be used. Both methods may become difficult in practice; increasing the amplitude may drift the system out of its linear operating range whereas increasing the number of injection periods requires more measurement time and computing power.

This paper proposes the use of the discrete-interval binary sequence (DIBS) for measuring the impedance of a Li-ion battery. The DIBS is a computer-optimized broadband binary signal where the optimization goal is to force as much power as possible into the specified harmonic frequencies without increasing the signal time-domain amplitude [6]. The frequency resolution is hence weakened but otherwise the DIBS has the same attractive properties as the conventional PRBS. Experimental measurements based on a commercial Li-ion battery are presented and used to demonstrate the effectiveness of the proposed method.

The remainder of the paper is organized as follows. Section II provides the theoretical background for characterizing battery state parameters based on the internal impedance. Section III presents the methods for battery impedance measurement. Section IV presents experimental measurements based on a commercial Li-ion battery. Finally, Section V draws conclusions.

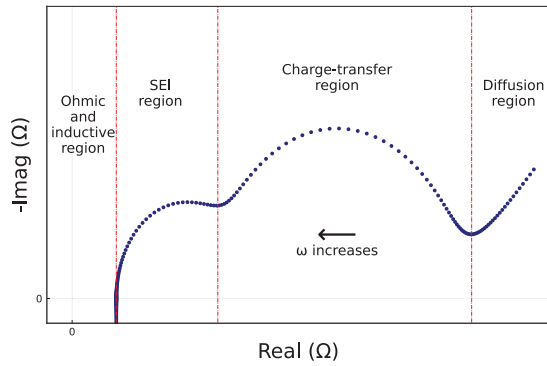


Fig. 1: Nyquist plot of a Li-ion battery impedance.

II. THEORY

The battery internal impedance has been shown to provide key information of the battery conditions. Fig. 1 shows a typical impedance spectra of a Li-ion battery as a Nyquist plot. The imaginary axis is most often inverted so that the capacitive characteristic of the impedance is shown in the first quadrant of the complex plane. The curve can be divided into different regions that signify different electrochemical processes in the battery. At low frequencies, typically less than a few hundreds mHz, diffusion processes dominate the electrodes and are represented by a 45° rising line in the Nyquist plot. In the mid-frequency region, ranging between several mHz to a few kHz, semicircular arches representing the charge-transfer (CT) region and the solid-electrolyte interphase (SEI) region characterize the movement of ions between the electrodes, the SEI layers and the electrolyte. At higher frequencies, the impedance values start to enter the ohmic and inductive region where the inductive behavior describes the overall dynamics for the conduction parts of the battery.

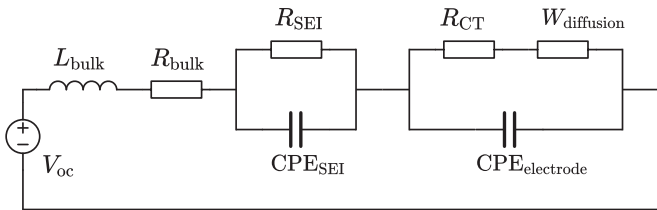


Fig. 2: Li-ion battery equivalent circuit model.

Studies have shown that changes in the Li-ion battery internal impedance closely relate to the changes of the battery state parameters such as SOC, SOH and temperature [7]. A popular approach in Li-ion battery impedance analysis involves forming of a battery equivalent circuit model (ECM) and fitting the impedance measurement data to obtain the ECM parameters [8]. Fig. 2 shows an example of a battery modeled by an equivalent circuit comprising of an open-circuit voltage source (V_{oc}) and passive electrical analogs. As seen in the circuit diagram, the battery dynamic characteristics in different ranges of frequency can be approximated by using a bulk resistor (R_{bulk}) and a bulk inductance (L_{bulk}) for the

ohmic and inductive region, a parallel circuit of a resistor (R_{SEI}) and a constant-phase element (CPE_{SEI}) for the SEI region, a combination of a resistor (R_{CT}), a Warburg element ($W_{diffusion}$) and a constant-phase element ($CPE_{electrode}$) for the CT and diffusion regions [9], [10]. Changes in the ECM parameter values have been demonstrated to correlate well with the battery SOC and SOH [4], [11]–[16]. Experiments have also examined the interdependency between the battery state parameters to show that the states can be reliably determined based on the impedance analysis [3], [16].

III. METHODS

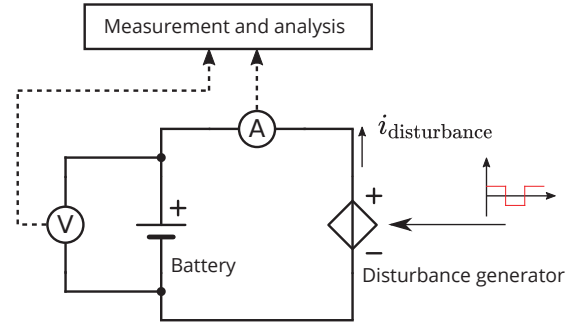


Fig. 3: Conceptual battery impedance measurement setup.

The basic principle for the battery internal impedance measurement is demonstrated in Fig. 3. In the diagram, an external current disturbance is applied to charge and discharge the battery. This process produces a voltage response at the battery terminals. The resulting current and output voltage are measured, and Fourier transform is applied to obtain the spectral information of the impedance. In practice, the measurements are typically averaged over a number of perturbation periods to reduce the effect of noise.

A. Broadband impedance measurement

A battery impedance is conventionally measured by applying the EIS [10]. In EIS, external sinusoidal current waves at various frequencies are sequentially applied to the battery terminals in accordance with Fig. 3. The EIS typically provides accurate impedance measurement results, but applying sinusoidal injections requires a relatively long measurement time. Another disadvantage of using sinusoids is that the signals contain a large number of different signal levels; implementing such signals is difficult in practice when low-cost devices are applied.

Recent studies have demonstrated methods based on broadband perturbations such as the PRBS to measure the battery impedance in a fraction of time compared to the EIS [5], [17]–[19]. The PRBS offers several attractive properties in real-time battery impedance measurement. The signal contains only two signal levels, and therefore, the signal can be implemented even with a low-cost signal generator the output of which can only cope with a small number of signal levels [20]. Compared to other perturbation signals the PRBS has a low peak factor which makes it suitable for measuring sensitive systems where

the system linear operation can be easily violated under high disturbance amplitude.

The problem in using the PRBS is that the signal energy is distributed over many harmonic frequencies, and the spectral-energy distribution is largely uncontrollable. If the perturbation energy needs to be increased, for example, due to strong external noise, either the perturbation amplitude needs to be increased or more periods of injection have to be applied with averaging. Increasing the amplitude can easily drift the system out of its linear operating range whereas increasing the number of injection periods requires longer measurement time and more computing power.

B. Discrete-interval binary sequence

The DIBS is one class of pseudo-random sequences where the signal is computer-optimized to force as much power as possible into the user-specified harmonic frequencies without increasing the signal time-domain amplitude [6]. Compared to the PRBS of the same length, the DIBS contains much higher power densities at the specified harmonics. An added benefit of the sequence is the freedom to customize the locations of the target frequency harmonics, for example, according to a logarithmic scale. Otherwise the DIBS has the same attractive properties as the conventional PRBS.

The optimization procedure for synthesizing the DIBS can be formulated as follows [21]–[24]. A sequence D_k is given as the discrete Fourier transform (DFT) of a signal d_n , where k denotes the harmonic index, n denotes the time-domain sample index ($0 \leq k < N$ and $1 \leq n \leq N$ where N denotes the length of D_k). The objective is now to find a sequence B_k so that the following cost function is minimized.

$$J = \sum_{k=0}^{N-1} (|D_k| - |B_k|)^2 \quad (1)$$

In (1), B_k represents the DFT of the optimized binary sequence b_n . In the beginning, the sequence b_n can be randomly assigned to any N -length binary sequence of unity amplitude. The DFT of b_n can then be calculated as

$$B_k = \sum_{n=1}^N b_n e^{-2\pi j \frac{n-1}{N} k} \quad \forall 0 \leq k < N$$

The phase angle sequence ϕ_k of B_k is extracted accordingly, as defined by

$$B_k = |B_k| e^{j\phi_k} \quad \forall 0 \leq k < N$$

Then, the sequence is further optimized by adjusting its phase angles ϕ_k in a series of loop iterations, where each iteration contains the following steps.

- 1) Create a complex-value sequence, defined as

$$C_k = |D_k| e^{j\phi_k} \quad \forall 0 \leq k < N$$

- 2) Obtain the inverse DFT of C_k as

$$c_n = \frac{1}{N} \sum_{k=0}^{N-1} C_k e^{2\pi j \frac{n-1}{N} k} \quad \forall 1 \leq n \leq N$$

- 3) Obtain a new binary sequence for b_n , by collecting the signs of c_n as

$$\forall 1 \leq n \leq N, \quad b_n = \begin{cases} 1 & \text{if } c_n > 0 \\ -1 & \text{if } c_n < 0 \\ \text{Either 1 or -1} & \text{if } c_n = 0 \end{cases}$$

- 4) Re-compute B_k and ϕ_k from the obtained b_n . Terminate the loop if the new ϕ_k remains unchanged compared to the phase values at the start of the current loop iteration. Otherwise, go back to the first step for the next iteration.

Finally, the optimization cost can be calculated using (1) and the latest values of B_k . Although the described iterative algorithm always guarantees convergence to a local minimum, that is, the loop always terminates at some point, the algorithm does not guarantee a globally optimal result. Therefore, several executions can be repeated with different random seed sequences for b_n so that multiple cost values are yielded to increase the likelihood of obtaining a globally minimum cost. It is also worth noting that typically only up to 85% of the signal total energy can be pushed into the specified harmonics [6].

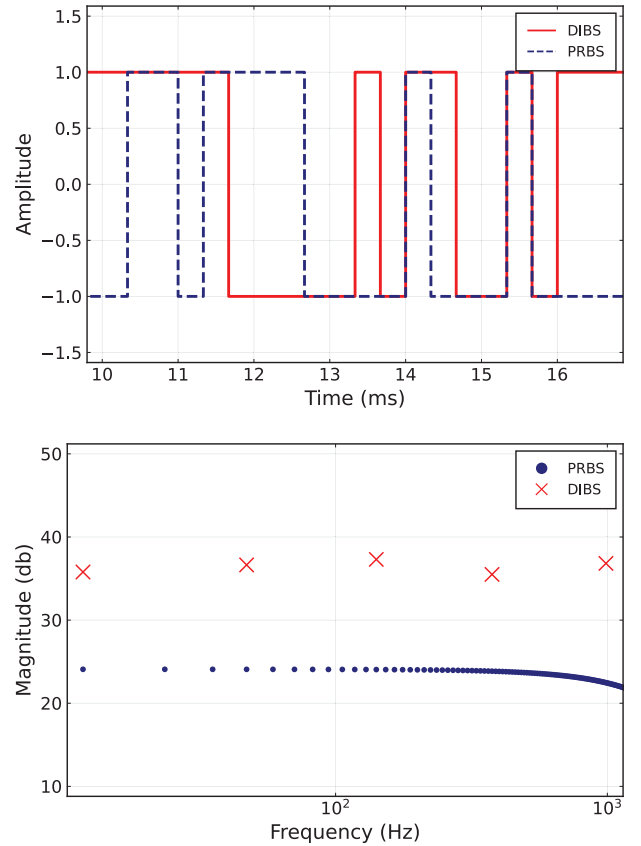


Fig. 4: PRBS and DIBS (5 harmonics) of length 255 and 3 kHz generation frequency in the a) time domain and b) frequency domain.

Fig. 4 shows samples of a PRBS and a DIBS of the same length (255 bits) and same generation frequency (3 kHz) in

both the time domain and the frequency domain. For the DIBS, five harmonic frequencies were logarithmically selected and the signal energy was maximized at these frequencies. Compared to the PRBS, the DIBS harmonics have approximately five times higher energy level in this example.

IV. EXPERIMENTS

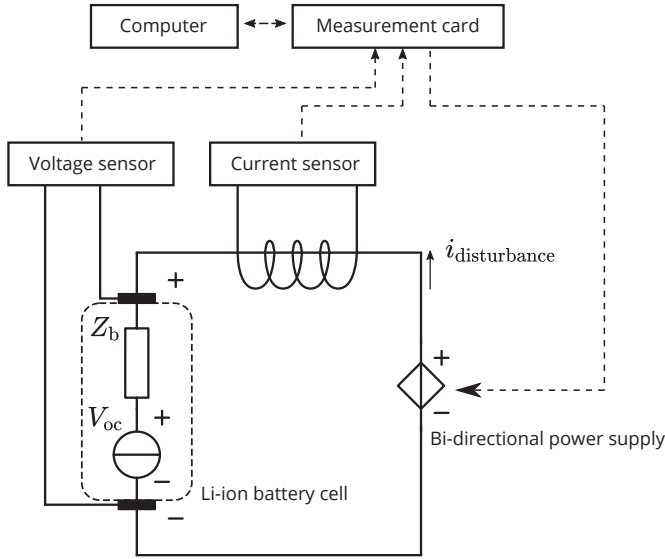


Fig. 5: Li-ion battery impedance measurement setup.

A measurement setup depicted in Fig. 5 was constructed to demonstrate the effectiveness of the proposed method. The system consists of a commercial Li-ion battery (TerraE INR 21700 50 E), a bi-directional power supply (Kepco BOP 50-20MG) for excitation injection, a measurement unit (NiDAQ USB-6363) for generating the excitation signal and collecting the data, and a computer for analyzing the data. The impedance was measured both by the conventional PRBS and the DIBS. Both signals had the same sequence length (8191 bits) and time-domain amplitude (0.025 A) but for the DIBS the spectral energy was maximized into 20 logarithmically selected frequency harmonics. Both signals were generated at 6 kHz. The sampling frequency of the measurement card was selected as 498 kHz. Table I shows the parameters of the used excitations.

TABLE I: Excitation variables

Variable name	PRBS	DIBS	Unit
Injection amplitude	0.025	0.025	A
Bandwidth	2	2	kHz
Generation frequency	6	6	kHz
Sequence length	8191	8191	bits
Frequency resolution	0.7325	1/10 decade	Hz
Number of injection periods	5	5	periods

The injections were separately applied so that the battery was charged and recharged according to the excitations. Fig. 6 shows samples of the measured current both in the time and

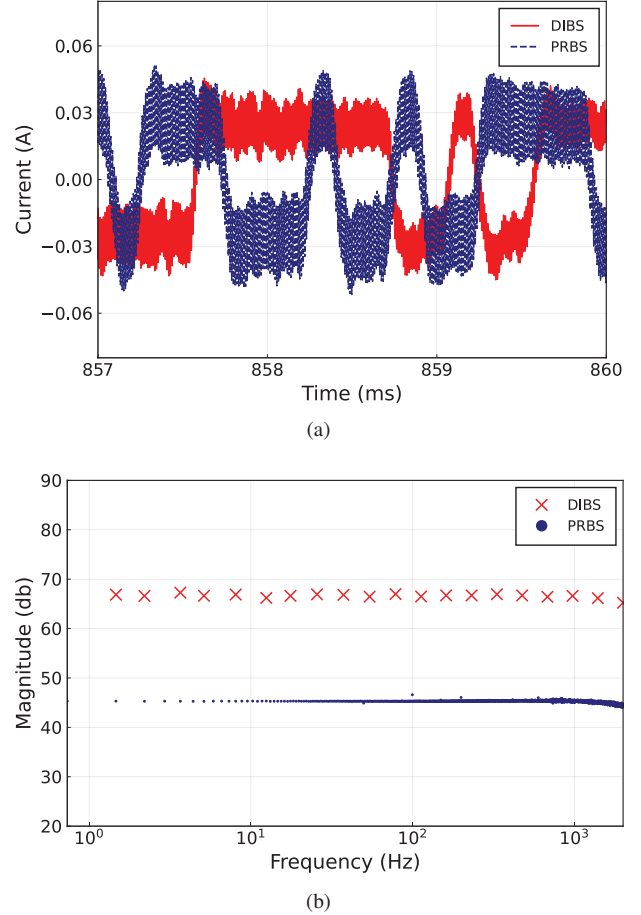


Fig. 6: Measured battery output current with PRBS and DIBS perturbations a) in the time domain and b) in the frequency domain.

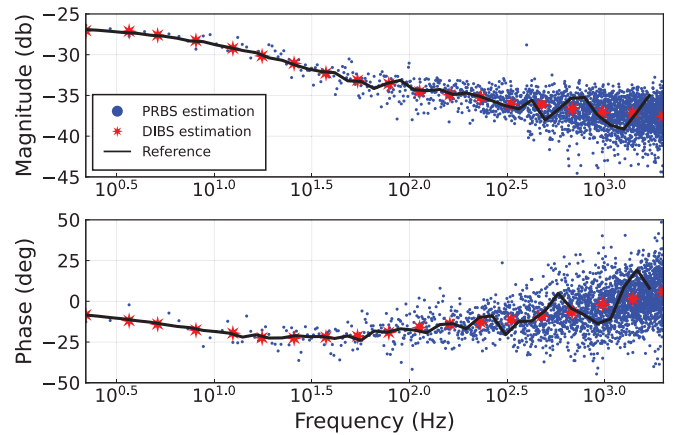


Fig. 7: Battery impedance Bode plot.

frequency domain. As the figure shows, the PRBS and the DIBS produce similar time-domain waveforms but the energy at the specified frequency harmonics is much higher (about 20 times) in the DIBS.

The measured current and voltage responses were Fourier transformed and averaged over the applied injection periods. Fig. 7 shows the computed impedance for both the PRBS and DIBS injections. The impedance was also measured by the EIS for obtaining a reference. As the figure shows, the impedance obtained by the DIBS highly accurately follows the reference whereas the impedance produced by the PRBS is strongly distorted in the whole frequency band. The results obtained by the PRBS could be improved by increasing the signal time-domain amplitude but this could easily drift the system out of its linear operating range.

V. CONCLUSION

Internal impedance is an important parameter in Li-ion battery health and charge estimation. Recent studies have demonstrated the application of the PRBS in online Li-ion battery impedance measurement. The method is able to accurately measure the impedance but it requires low noise floor.

This paper has proposed the use of the discrete-interval binary sequence (DIBS) to perform real-time battery-impedance measurements. The DIBS is a computer-optimized pseudo-random sequence in which the spectral energy can be maximized at user-specified frequency harmonics without increasing the signal time-domain amplitude. The signal is particularly useful for sensitive battery systems that can easily drift out from a linear operating range due to an external perturbation. Experiment results showed that the DIBS offers superior accuracy compared to the conventional PRBS.

The presented methods can be utilized in various applications of Li-ion batteries. One example could be defining the battery quality in real-time, for example, in electric vehicles. Another example could be performing mass testing to used batteries and defining their capability in second-life applications. The future work will consider the practical limitations of the method and implementing the technique in real-world applications.

REFERENCES

- [1] G. Zubi, R. Dufo-López, M. Carvalho, and G. Pasaoglu, "The lithium-ion battery: State of the art and future perspectives," *Renewable and Sustainable Energy Reviews*, vol. 89, pp. 292–308, 2018.
- [2] M. A. Hannan, M. M. Hoque, A. Hussain, Y. Yusof, and P. J. Ker, "State-of-the-art and energy management system of lithium-ion batteries in electric vehicle applications: Issues and recommendations," *IEEE Access*, vol. 6, pp. 19 362–19 378, 2018.
- [3] X. Wang, X. Wei, H. Dai, and Q. Wu, "State estimation of lithium ion battery based on electrochemical impedance spectroscopy with on-board impedance measurement system," in *Proc. IEEE Vehicle Power and Propulsion Conference*, 2015, pp. 1–5.
- [4] D. N. T. How, M. A. Hannan, M. S. Hossain Lipu, and P. J. Ker, "State of charge estimation for lithium-ion batteries using model-based and data-driven methods: A review," *IEEE Access*, vol. 7, pp. 136 116–136 136, 2019.
- [5] J. Sihvo, D.-I. Stroe, T. Messo, and T. Roinila, "Fast approach for battery impedance identification using pseudo-random sequence signals," *IEEE Transactions on Power Electronics*, vol. 35, no. 3, pp. 2548–2557, 2020.
- [6] K. Godfrey, "Design and application of multifrequency signals," *Computing & Control Engineering Journal*, vol. 2, no. 4, pp. 187–195, 1991.
- [7] M. A. Hannan, M. H. Lipu, A. Hussain, and A. Mohamed, "A review of lithium-ion battery state of charge estimation and management system in electric vehicle applications: Challenges and recommendations," *Renewable and Sustainable Energy Reviews*, vol. 78, pp. 834–854, 2017.
- [8] X. Wang, X. Wei, J. Zhu, H. Dai, Y. Zheng, X. Xu, and Q. Chen, "A review of modeling, acquisition, and application of lithium-ion battery impedance for onboard battery management," *eTransportation*, vol. 7, p. 100093, 2021.
- [9] W. Choi, H.-C. Shin, J. M. Kim, J.-Y. Choi, and W.-S. Yoon, "Modeling and applications of electrochemical impedance spectroscopy (eis) for lithium-ion batteries," *Journal of Electrochemical Science and Technology*, vol. 11, no. 1, pp. 1–13, 2020.
- [10] D. D. Macdonald, "Reflections on the history of electrochemical impedance spectroscopy," *Electrochimica Acta*, vol. 51, no. 8-9, pp. 1376–1388, 2006.
- [11] N. Chen, P. Zhang, J. Dai, and W. Gui, "Estimating the state-of-charge of lithium-ion battery using an h-infinity observer based on electrochemical impedance model," *IEEE Access*, vol. 8, pp. 26 872–26 884, 2020.
- [12] A. Eddahech, O. Briat, N. Bertrand, J.-Y. Delétage, and J.-M. Vinassa, "Behavior and state-of-health monitoring of li-ion batteries using impedance spectroscopy and recurrent neural networks," *International Journal of Electrical Power & Energy Systems*, vol. 42, no. 1, pp. 487–494, 2012.
- [13] M. Kassem, J. Bernard, R. Revel, S. Pelissier, F. Duclaud, and C. Delacourt, "Calendar aging of a graphite/lifepo4 cell," *Journal of Power Sources*, vol. 208, pp. 296–305, 2012.
- [14] H.-F. Yuan and L.-R. Dung, "Offline state-of-health estimation for high-power lithium-ion batteries using three-point impedance extraction method," *IEEE Transactions on Vehicular Technology*, vol. 66, no. 3, pp. 2019–2032, 2016.
- [15] U. Tröltzsch, O. Kanoun, and H.-R. Tränkler, "Characterizing aging effects of lithium ion batteries by impedance spectroscopy," *Electrochimica acta*, vol. 51, no. 8-9, pp. 1664–1672, 2006.
- [16] D. I. Stroe, M. Swierczynski, A. I. Stan, V. Knap, R. Teodorescu, and S. J. Andreasen, "Diagnosis of lithium-ion batteries state-of-health based on electrochemical impedance spectroscopy technique," in *Proc. IEEE Energy Conversion Congress and Exposition*, 2014, pp. 4576–4582.
- [17] E. Locorotondo, S. Scavuzzo, L. Pugi, A. Ferraris, L. Berzi, A. Airale, M. Pierini, and M. Carello, "Electrochemical impedance spectroscopy of li-ion battery on-board the electric vehicles based on fast nonparametric identification method," in *Proc. IEEE International Conference on Environment and Electrical Engineering and IEEE Industrial and Commercial Power Systems Europe*, 2019, pp. 1–6.
- [18] J. Sihvo, T. Roinila, and D.-I. Stroe, "Broadband impedance measurement of lithium-ion battery in the presence of nonlinear distortions," *Energies*, vol. 13, no. 10, 2020.
- [19] A. Fairweather, M. Foster, and D. Stone, "Battery parameter identification with pseudo random binary sequence excitation (prbs)," *Journal of Power Sources*, vol. 196, no. 22, pp. 9398–9406, 2011.
- [20] K. Godfrey, "Introduction to binary signals used in system identification," in *Proc. International Conference on Control*, 1991, pp. 161–166.
- [21] A. V. D. BOS and R. Krol, "Synthesis of discrete-interval binary signals with specified fourier amplitude spectra," *International Journal of Control*, vol. 30, no. 5, pp. 871–884, 1979.
- [22] M. Buckner and T. Kerlin, "Optimum binary signals for reactor frequency response measurements," *Nuclear Science and Engineering*, vol. 49, no. 3, pp. 255–262, 1972.
- [23] K.-D. Paehlike and H. Rake, "Binary multifrequency signals-synthesis and application," *IFAC Proceedings Volumes*, vol. 12, no. 8, pp. 589–596, 1979.
- [24] S. L. Harris and D. A. Mellichamp, "On-line identification of process dynamics: use of multifrequency binary sequences," *Industrial & Engineering Chemistry Process Design and Development*, vol. 19, no. 1, pp. 166–174, 1980.